AN ANALYSIS OF SAMPLING FOR FILTER-BASED FEATURE EXTRACTION AND ADABOOST LEARNING

Anselm Haselhoff and Anton Kummert
Communication Theory, University of Wuppertal, 42097 Wuppertal, Germany

Keywords: Feature extraction, Sampling, AdaBoost.

Abstract: In this work a sampling scheme for filter-based feature extraction in the field of appearance-based object detection is analyzed. Optimized sampling radically reduces the number of features during the AdaBoost training process and better classification performance is achieved. The signal energy is used to determine an appropriate sampling resolution which then is used to determine the positions at which the features are calculated. The advantage is that these positions are distributed according to the signal properties of the training images.

The approach is verified using an AdaBoost algorithm with Haar-like features for vehicle detection. Tests of classifiers, trained with different resolutions and a sampling scheme, are performed and the results are presented.

1 INTRODUCTION

Video cameras facilitate application of various object detection algorithms and especially appearance-based methods gained interest since they are generally applicable to object detection problems. These methods learn the characteristics of vehicle appearance from a set of training images which capture the variability in the vehicle class (Sun et al., 2004). Different combinations of feature extraction methods and learning algorithms are proposed (Sun et al., 2004), (Ponsa et al., 2005) to form an appearance-based object detection system.

The object detection system proposed by Viola & Jones (Viola and Jones, 2001) is one of the most frequently used systems (e.g. (Lienhart et al., 2002), (Ponsa et al., 2005), (Overett and Petersson, 2007)). The competitive edge is reached by means of the fast computation of the Haar-like features and the cascaded structure of the classifier. These facts make the system work in real-time.

The system relies on a unified image resolution to guarantee a comparable number of features to be extracted, where unified means that all images used for training have the same resolution. This choice of resolution is highly related to sampling. Obviously using a too low resolution leads to a lack of important information and in turn unsatisfying classification results are obtained. In contrast, using a very high resolution the learning algorithm has to cope with the risk of concentrating on too specific object properties and the computational load grows rapidly.

The scale selection of the features, which is ’equivalent’ to image scale selection, is implicitly done by the feature selector that chooses the size of the Haar-like features. Thus, the task is rather to offer the feature selector included in the learning algorithm a wide range of possible feature scales which capture the most information of the training data while preserving low computational complexity.

The image resolution can be explicitly changed by resizing the images or implicitly changed by scaling the features and calculate them at certain sampling positions. Concerning the latter case, the obvious solution is to use equally-spaced sampling positions in horizontal and vertical direction. This is just a specific case of multidimensional sampling where no mutual dependency between different dimensions is considered. The dependencies between different dimensions can be used to improve the efficiency of the sampling in terms of the number of sampling points.

In this work a sampling methodology is presented that can be adjusted to the training data at hand and different sampling options are exposed. On the one hand the number of sampling points can be reduced while preserving the same signal energy and on the

Haselhoff A. and Kummert A. (2009).
AN ANALYSIS OF SAMPLING FOR FILTER-BASED FEATURE EXTRACTION AND ADABOOST LEARNING.
In *Proceedings of the Fourth International Conference on Computer Vision Theory and Applications*, pages 180-185
DOI: 10.5220/0001791201800185

other hand the number of sampling points can be fixed, but by means of a different sampling scheme more energy is preserved.

The remainder of the paper proceeds as follows. Firstly, section 2 gives a brief description of the used learning algorithm and features. Secondly, in section 3 the key ideas of 2D sampling are summarized. Next, in section 4 the sampling methodology is presented and finally, the results of trained classifiers with different training resolutions and the sampling scheme are presented. The classification accuracy confirms the advantages of the presented sampling scheme.

2 DETECTION ALGORITHM

2.1 Haar-like Features

In the object detection system developed by Viola & Jones (Viola and Jones, 2001) Haar-like features are proposed, called rectangle features. The advantage of these features is a very fast computation due to the use of the integral image.

For the training process, an exhaustive set of features is used from which the AdaBoost algorithm can select the most important ones. The feature values are obtained by applying the filters in different scales to varying positions on an image. The five basic types of rectangular filter masks (band-pass filters) are shown in figure 1.

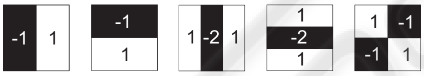

Figure 1: Five basic types of rectangular filter masks.

2.2 The Boosting Algorithm

The feature representation is used for the training of the classifier by means of an AdaBoost algorithm. AdaBoost performs a feature selection and combines the selected features as simple weak classifiers to a strong one. In each iteration step of the AdaBoost algorithm the weak classifier with the smallest weighted classification error is selected. Each weak classifier is dependent on just one component of the feature vector and the classification is done via a simple threshold comparison.

A strong classifier is trained with the discrete AdaBoost (Viola and Jones, 2001) algorithm and is defined as

$$H(\mathbf{x}) = \begin{cases} 1, & \sum_{t=1}^{T} \alpha_t h_t(\mathbf{x}) \geq \frac{1}{2} \sum_{t=1}^{T} \alpha_t \\ 0, & \text{otherwise} \end{cases},$$

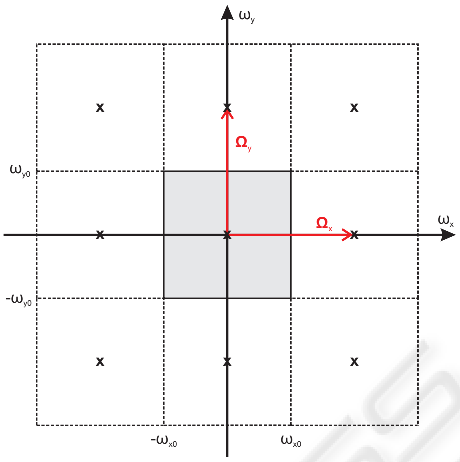

Figure 2: Rectangular sampling in the frequency domain. Grayish area denotes the rectangular base band and dashed lines denote the spectral copies. ω_{x0} and ω_{y0} are the cut-off frequencies in x- and y- direction respectively. The sampling frequency matrix $\mathbf{\Omega}_{rect}$ is constructed using the vectors $\mathbf{\Omega}_x$ and $\mathbf{\Omega}_y$.

where $\mathbf{x}$ is the feature vector of an image, $h_t \in \{0,1\}$ is a weak classifier, α_t is the weight of the t-th weak classifier and T is the number of features selected. The weak classifiers are combined by a weighted majority vote to a strong classifier H.

After the offline learning process only a few selected features must be calculated for online classification.

3 SAMPLING OF 2D SIGNALS

3.1 Naming Conventions and Basics

In the following sections $f(x,y) = f(\mathbf{r})$ denotes a 2D singal or image with $\mathbf{r} = (x,y)^T$, where a superscript T denotes transposition. The same shorthand notation is used for the Fourier transform.

For a 2D continuous function $f(\mathbf{r})$ the Fourier transform $F(j\boldsymbol{\omega}) \bullet\!\!-\!\!\circ f(\mathbf{r})$ with $\boldsymbol{\omega} = (\omega_x, \omega_y)^T$ is defined as

$$f(\mathbf{r}) = \frac{1}{(2\pi)^2} \int_{\mathbb{R}^2} F(j\boldsymbol{\omega}) e^{j\boldsymbol{\omega}^T \mathbf{r}} d\boldsymbol{\omega} \quad (1)$$

$$F(j\boldsymbol{\omega}) = \int_{\mathbb{R}^2} f(\mathbf{r}) e^{-j\boldsymbol{\omega}^T \mathbf{r}} d\mathbf{r}. \quad (2)$$

3.2 2D Sampling

The transition from 1D to 2D signals, like images, comes along with new concepts related to sampling.

These concepts are caused by the mutual dependencies across different dimensions. In 2D the sampling period becomes a sampling matrix

$$\mathbf{T} = \begin{bmatrix} T_{11} & T_{12} \\ T_{21} & T_{22} \end{bmatrix} = (\mathbf{T}_x, \mathbf{T}_y).$$

The sampled signal $f_S(\mathbf{r})$ and the continuous signal $f(\mathbf{r})$ are then connected by

$$f_S(\mathbf{r}) = \sum_{\mathbf{n}\in\mathbb{Z}^2} f(\mathbf{Tn})\,\delta(\mathbf{r}-\mathbf{Tn}). \quad (3)$$

In analogy with the 1D case, the relation of the sampling matrix $\mathbf{T}$ and the sampling frequency $\mathbf{\Omega}$ is given by

$$\mathbf{\Omega} = 2\pi\left(\mathbf{T}^T\right)^{-1}, \quad (4)$$

where $\mathbf{\Omega}$ is a matrix as well with

$$\mathbf{\Omega} = \begin{bmatrix} \Omega_{11} & \Omega_{12} \\ \Omega_{21} & \Omega_{22} \end{bmatrix} = (\mathbf{\Omega}_x, \mathbf{\Omega}_y).$$

This sampling frequency matrix $\mathbf{\Omega}$ defines where the spectral copies of the base band are located. Depending on the spectral properties of the signal at hand an appropriate sampling scheme can be chosen. In Ohm (Ohm, 2004) the following sampling schemata are discussed: rectangular, shear, hexagonal, and quincunx sampling. The simplest option is the rectangular sampling with a fixed step-width T for both directions, so that

$$\mathbf{T} = T\begin{bmatrix} 1 & 0 \\ 0 & 1 \end{bmatrix}. \quad (5)$$

The sampling can be adjusted to the signal properties for each direction. For example if an image signal has high frequency components in the x-dimension and a very fine-grained sampling has to be chosen, this is not necessarily required for the y-dimension. This is an important aspect since images are generally resized preserving the same width to height ratio.

The impact of rectangular sampling with the base band and its periodic replications are visualized in figure 2. The width to height ratio is not fixed and ω_{x0} and ω_{y0} are the cut-off frequencies in x- and y-dimension respectively. The resulting sampling frequency is then

$$\mathbf{\Omega}_{rect} = \begin{bmatrix} 2\omega_{x0} & 0 \\ 0 & 2\omega_{y0} \end{bmatrix} = (\mathbf{\Omega}_x, \mathbf{\Omega}_y).$$

Using equation 4 the appropriate sampling matrix can be obtained

$$\mathbf{T}_{rect} = \begin{bmatrix} \pi/\omega_{x0} & 0 \\ 0 & \pi/\omega_{y0} \end{bmatrix}.$$

The difference between 1D and 2D sampling is that the sampling positions of one dimension can be chosen depending on those of another dimension (non separable sampling). For example the quincunx sampling (Ohm, 2004) is a none separable sampling, where the shape of the base band is rhombus like. Figure 3 shows a rhombus shaped base band and the according periodic replications. It is obvious that one possible solution to get the sampling frequency matrix is to choose $\mathbf{\Omega}_x = (2\omega_{x0}, 0)^T$ and $\mathbf{\Omega}_y = (\omega_{x0}, \omega_{y0})^T$. As a result the sampling frequency is

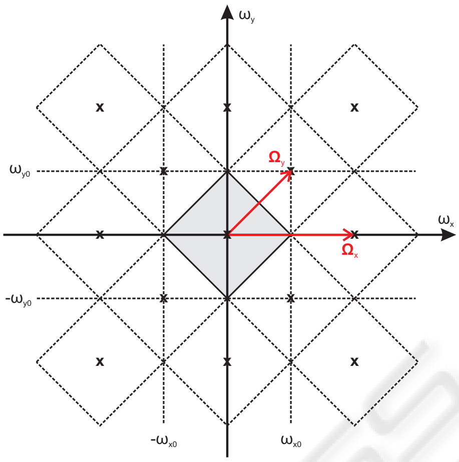

Figure 3: Quincunx sampling in the frequency domain. Grayish area denotes the rhombus-like base band and dashed lines denote the spectral copies. ω_{x0} and ω_{y0} are the cut-off frequencies in x- and y- direction respectively. The sampling frequency matrix $\mathbf{\Omega}_{quin}$ is constructed using the vectors $\mathbf{\Omega}_x$ and $\mathbf{\Omega}_y$.

$$\mathbf{\Omega}_{quin} = \begin{bmatrix} 2\omega_{x0} & \omega_{x0} \\ 0 & \omega_{y0} \end{bmatrix}$$

and the corresponding sampling matrix is given by

$$\mathbf{T}_{quin} = \begin{bmatrix} \pi/\omega_{x0} & 0 \\ -\pi/\omega_{y0} & 2\pi/\omega_{y0} \end{bmatrix}.$$

3.3 Signal Energy in 2D

Generally, it can be assumed that using sampling means losing information. To get an idea of how crucial this error is, the energy can be regarded. The energy of a signal $f(\mathbf{r})$ is defined as

$$E = \int_{\mathbb{R}^2} |f(\mathbf{r})|^2\, d\mathbf{r}. \quad (6)$$

Parseval's theorem (Ohm, 2004) can be used to measure the energy in the frequency domain

$$\int_{\mathbb{R}^2} |f(\mathbf{r})|^2\, d\mathbf{r} = \frac{1}{(2\pi)^2}\int_{\mathbb{R}^2} |F(j\boldsymbol{\omega})|^2\, d\boldsymbol{\omega}. \quad (7)$$

With these equations a measure to assess the signal energy that is preserved in a sampled signal can be defined. The energy of the sampled signal can be approximated by

$$E_D = \frac{1}{(2\pi)^2} \int_D |F(j\boldsymbol{\omega})|^2 \, d\boldsymbol{\omega}. \tag{8}$$

D denotes a set which is determined by the cut-off frequencies and the sampling method. For a rectangular sampling the set can be defined as follows

$$D_{rect} = \left\{ \begin{pmatrix} \omega_x \\ \omega_y \end{pmatrix} \in \mathbb{R}^2 \middle| |\omega_x| \le \omega_{x0} \wedge |\omega_y| \le \omega_{y0} \right\}.$$

Analogously a set for the quincunx sampling can be derived as

$$D_{quin} = \left\{ \begin{pmatrix} \omega_x \\ \omega_y \end{pmatrix} \in \mathbb{R}^2 \middle| \frac{|\omega_x|}{\omega_{x0}} + \frac{|\omega_y|}{\omega_{y0}} \le 1 \right\}.$$

Finally, the energy packing efficiency η_D of a sampled signal can be defined as the relative portion of the energy that is preserved in the sampled signal. This ratio of energy E_D and the energy E_{ref} of a reference signal (e.g. the energy E of the continuous signal) is a measure to compare different sampling rates.

$$\eta_D = \frac{E_D}{E_{ref}} \tag{9}$$

4 2D SAMPLING FOR IMAGE FEATURE EXTRACTION

In general, the camera parameters and the distance in which each training image was collected would be needed to determine the sampling matrix and thus enable the usage of the equations from section 3. For our experiments it is assumed that this information is not available. Therefore no information about the sampling period in world coordinates is given and some assumptions have to be made. It is assumed that the resolution $M \times N$ is the highest possible resolution. Generally speaking, this is the highest image resolution that can be found in the trainingset. This image resolution is used as the reference resolution which is our optimal case and takes the place of our continuous signal.

The proposed sampling approach is divided into two parts. The goal of the first part is to get those parameters that are necessary to calculate the sampling matrix in the second part. These are either the number of sampling points or the energy packing efficiency. Firstly, a reasonable training resolution $M' \times N'$ has to be defined. Therefore the approach presented in [] can be used or a fixed resolution can be set in advance (e.g. 32×24 for vehicle detection). At this point the energy packing efficiency for this specific resolution has to be calculated in reference to $M \times N$ using the equations from section 3. To reach this goal all training images are resized to the maximal resolution of $M \times N$ and afterwards the mean value of the discrete Fourier transform (DFT) is calculated. The DFT is then used in combination with equation 8 and D_{rect} to determine the energy packing efficiency for the resolution $M' \times N'$. In this context, the cut-off frequencies are directly connected to the resolution using rectangular sampling. For the maximal resolution the cut-off frequencies are fixed, so that $\omega_{x0} = \pi$ and $\omega_{y0} = \pi$. The cut-off frequencies $\omega_{x0}^{'}$ and $\omega_{y0}^{'}$ for a downsampled image are then connected to $M' \times N'$ by

$$M' = \frac{\omega_{x0}^{'} M}{\pi} \tag{10}$$

and

$$N' = \frac{\omega_{y0}^{'} N}{\pi}. \tag{11}$$

Thus, the sampling frequency $\boldsymbol{\Omega}_{rect}$ and the energy packing efficiency η_D can be obtained for all resolutions up to $M \times N$.

In the second part an optimized sampling matrix has to be determined e.g. for quincunx sampling $\mathbf{T}_{quin}$. To find this sampling matrix one of two optimization constraints can be chosen. The first one is to use the energy packing efficiency, so that the new sampling matrix leads to the same value of η_D that was defined in the first part, but using fewer sampling positions. These positions are distributed according to the signal properties of the images. The second option is to use the same number of sampling points and find an arrangement of sampling points that preserve more energy. In this paper the first option is discussed.

The procedure is almost the same as in part one. The difference lies in the aspect how the sampling matrix is determined. Now, equation 8 and D_{quin} is used for all different combinations of $\omega_{x0}^{'}$ and $\omega_{y0}^{'}$. Thus for all combinations the energy packing efficiency can be calculated. Afterwards these values for $\omega_{x0}^{'}$ and $\omega_{y0}^{'}$ are chosen whoes corresponding energy efficiency value is closest to the predefined value η_D and which would result in the lowest number of sampling points. These sampling periods can then be used to generate a sampling grid which serves as a rule where the Haar-like features should be calculated.

5 RESULTS AND CONCLUSIONS

In this section the results provided by the proposed approach described in the previous sections are discussed and the performance results of the trained classifiers are presented. As already mentioned the object detection system developed by Viola & Jones (Viola and Jones, 2001) is used to verify the approach. The trainingset consists of 2600 vehicle rear view images as positive samples and 7007 other images as negative samples, whereas the independent testset comprises 1114 vehicle rear views and 3003 negative samples. These manually labeled images are collected from the Label-Me (Russell et al., 2005) database. To enable the Haar-like features to capture the edges of the vehicles ten percent of the background is added at the edges of the images.

For this training- and testset the maximal resolution $M \times N$ is 256×192, with the same width to height ratio as presented in (Ponsa et al., 2005). Now the energy packing efficiency for different resolutions $M' \times N'$ up to 256×192 can be calculated. Fig. 4 shows the energy packing efficiency for progressively increasing resolution. For a width smaller than 20 pixels the energy is rapidly decreasing, hence choosing a resolution higher than 20×15 is reasonable. In this work a training resolution of 32×24 is chosen, which is intentionally large compared to other experimental results (e.g. (Ponsa et al., 2005), (Lienhart et al., 2002)).

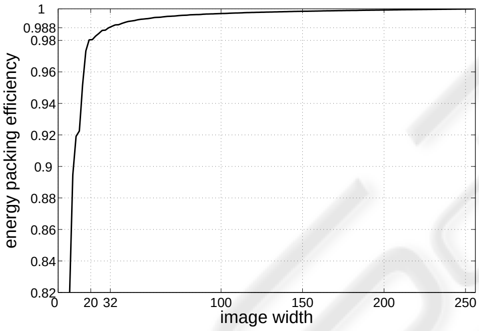

Figure 4: Energy packing efficiency for progressively increasing resolution.

For this resolution $\eta_D = 0.988$ is obtained, which means that 98.8% of the energy of the reference image with maximal resolution is preserved. The sampling matrix with reference to 256×192 is

$$\mathbf{T}_{rect} = \begin{bmatrix} 8 & 0 \\ 0 & 8 \end{bmatrix}.$$

By inspecting the DFT of the training images it becomes obvious that the high frequency components are rather located in the vertical direction (see fig. 5). This means that our vehicle training images contain many strong horizontal edges. This fact should be considered choosing a sampling scheme. It would be more effective to choose a high resolution in the vertical and a smaller resolution in the horizontal dimension. This is essentially the outcome of the optimization procedure from the last section with the quincunx sampling, where the algorithm is constrained to find a sampling matrix $\mathbf{T}$ which results in preserving 98.8% of the energy. Regarding the reference resolution, the optimal sampling scheme is given by

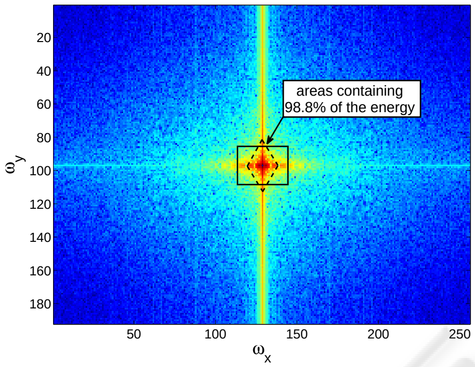

Figure 5: Rectangular and Quincunx base band for the training data preserving 98.8% of the energy. Rectangular and Quincunx sampling are denoted by the solid and dashed lines, respectively.

$$\mathbf{T}_{quin} = \begin{bmatrix} 12.8 & 0 \\ -6.4 & 12.8 \end{bmatrix}.$$

The corresponding base bands for rectangular and quincunx sampling are shown in figure 5. The quincunx sampling is marked by the dashed line and the rectangular sampling is marked by the solid line. Since both methods cover the same energy of the image signals the interesting part is the reduction in sampling points. For the resolution of 32×24 the number of sampling points is 768 and for the quincunx sampling the number is reduced by more than 50% to just 300 sampling points. The sampling grids for both methods are visualized in figure 6. The advantage of the quincunx sampling is that mutual dependencies across the x- and y-dimension are considered and that a higher resolution in vertical than in horizontal dimension is achieved.

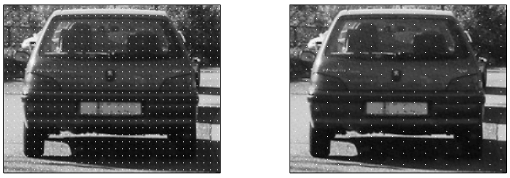

(a) Rectangular sampling (b) Quincunx sampling

Figure 6: Rectangular (768 sampling points) and Quincunx (300 sampling points) sampling grid.

For the evaluation, three classifiers are trained using an AdaBoost algorithm with the same training parameters. All classifiers have 100 features and the difference between these classifiers is the training image resolution. Two classifiers are trained by resizing the images to a resolution of 16×12 and 32×24, respectively. For these classifiers the sampling matrix is

$$\mathbf{T}_{rect} = \begin{bmatrix} 1 & 0 \\ 0 & 1 \end{bmatrix}.$$

This sampling matrix is common practice and means that the five Haar-like features (Fig. 1) are calculated at all image coordinates.

The third classifier uses the quincunx sampling method. To perform this sampling, a minimal resolution of 40×30 is required. After resizing the image just these positions are used for feature calculation which are determined by the quincunx sampling matrix

$$\mathbf{T}_{quin} = \begin{bmatrix} 2 & 0 \\ -1 & 2 \end{bmatrix}.$$

It is to mention that the minimal size of the Haar-like features is set to be 2×2. Table 1 shows the number of sampling points and features that are extracted during the training process. The performance results of the different classifiers are illustrated by using ROC curves as shown in Fig. 7. The results reveal that the best classification performance is obtained by using the resolution 40×30 with the sampling method and unsatisfying performance by the resolution 16×12. Even though the best classifier's feature pool is significantly smaller than the number of features used for the classifier with resolution 32×24 the results are slightly better. This strengthens the assumption that the proposed sampling method is valid and moreover can even improve classification performance without increasing the computational load during the training process.

Table 1: Trained classifiers.

Resolution	Sampling Points	Features
16×12, $\mathbf{T}_{rect}$	192	$15 \cdot 10^3$
32×24, $\mathbf{T}_{rect}$	768	$260 \cdot 10^3$
40×30, $\mathbf{T}_{quin}$	300	$160 \cdot 10^3$

Summing up, an approach has been introduced to generate a sampling grid to determine reasonable positions for calculating the Haar-like features. On the one hand the number of features is reduced by around 40% and the classification accuracy is increased. These advantages are due to the better utilization of positions for feature calculation which are adapted to the properties of the training images. One aspect that should be included in future work is to transfer this methodology directly to the Haar-like features to further reduce the computational complexity without losings in accuracy.

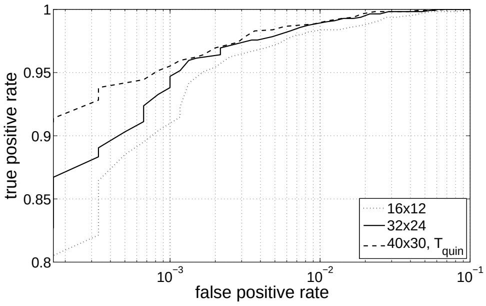

Figure 7: ROC curve of three equally trained classifiers using two different cartesian and the quincunx sampling.

REFERENCES

Lienhart, R., Kuranov, A., and Pisarevsky, V. (2002). Empirical analysis of detection cascades of boosted classifiers for rapid object detection. Technical report, Mic. Research Lab, Intel Corporation, Santa Clara, CA 95052, USA.

Ohm, J.-R. (2004). *Multimedia Communication Technology*. Springer, Berlin, Heidelberg, Germany.

Overett, G. and Petersson, L. (2007). Boosting with multiple classifier families. *Proc. of IEEE Intelligent Vehicles Symposium*, pages 1039–1044.

Ponsa, D., Lopez, A., Lumbreras, F., Serrat, J., and Graf, T. (2005). 3d vehicle sensor based on monocular vision. In *Proc. of the 8th Int. IEEE Conf. on Intelligent Transportation Systems*, Vienna, Austria.

Russell, B., Torralba, A., and Freeman, W. T. (2005). Labelme image database. http://labelme.csail.mit.edu.

Sun, Z., Bebis, G., and Miller, R. (2004). On-road vehicle detection using optical sensors: A review.

Viola, P. and Jones, M. (2001). Rapid object detection using a boosted cascade of simple features. In *Accepted Conf. on Computer Vision and Pattern Recognition*.